Tetrahedron 70 (2014) 5420–5427

Contents lists available at ScienceDirect

Tetrahedron

journal homepage: www.elsevier.com/locate/tet

New cyclic RGD peptides: synthesis, characterization, and theoretical activity towards $\alpha_v\beta_3$ integrin

Helena Vilaça, Paula M.T. Ferreira *, Nuno M. Micaelo

Chemistry Centre, University of Minho, Campus de Gualtar, 4710-057 Braga, Portugal

ARTICLE INFO

Article history:
Received 10 April 2014
Received in revised form 18 June 2014
Accepted 30 June 2014
Available online 3 July 2014

Keywords:
Cyclic RGD
Bis-azides
Click chemistry
Integrin $\alpha_v\beta_3$
Docking experiments

ABSTRACT

Two new cyclic RGD peptides were prepared using a click chemistry approach. The linear RGDfV peptide was synthesized by solid-phase peptide synthesis using a 9-fluorenylmetoxicarbonyl (Fmoc) strategy and a 2-chlorotrityl chloride resin. After coupling 5-hexynoic acid the peptide was cleaved from the resin and linked to propargylamine. The bis-alkynyl RGDfV peptide was then reacted with two different bis-azides by treatment with copper iodide and triethylamine. These two cyclic RGD peptides were characterized by NMR and HRMS. In order to evaluate the interaction of these new compounds with integrin $\alpha_v\beta_3$ docking experiments were carried out and the results compared with those obtained with *cyclo*(RGDf[N–Me]V) (Cilengitide). The two new cyclic RGD peptides showed a higher affinity to the $\alpha_v\beta_3$ integrin when compared with Cilengitide thus representing two new potential integrin $\alpha_v\beta_3$ antagonists.

1. Introduction

Arginine-Glycine-Aspartic acid (RGD) is a sequence present in various extracellular matrix adhesion proteins such as vitronectin, fibrinogen, fibronectin or osteopontin. The sequence is responsible for the interactions of these proteins with a group of cell-surface receptors called integrins.[1,2] Integrins are involved in important cellular processes namely in cellular proliferation and in apoptosis.[3] Integrin $\alpha_v\beta_3$ is a member of this family of cellular receptors and is over-expressed in activated endothelial cells in the neovasculature of tumors and in some solid tumors.[4] Angiogenesis is essential in the growth of solid tumors and in the development of metastases.[1] Several integrin subtypes recognize the sequence RGD. However, receptor selectivity exists for distinct natural ligands. One reason given for this selectivity is the different conformations adopted by the RGD sequence, which are defined by the protein/peptide structure.[5] Thus, research has focused on the synthesis and development of $\alpha_v\beta_3$ inhibitors, particularly peptides containing the RGD sequence with restrict conformational space.[5–10]

Several structure–activity relationship studies between peptides with the RGD sequence and integrin $\alpha_v\beta_3$ have been carried out.[1,6,11–14] Pierschbacher et al.[13] found that the substitution of the RGD sequence for analogue amino acids or for the D-enantiomers decreased the affinity of peptides for this integrin. This study also showed that the affinity of cyclic peptides is much higher when compared with their linear counterparts. Kessler et al.[3,11,12,14,15] showed that cyclic hexa- and pentapeptides with the RGD sequence have greater selectivity for the $\alpha_v\beta_3$ integrin when the distance between the α and β carbon atoms of arginine and aspartic acid is 500 and 700 pm, respectively. The presence of a hydrophobic amino acid with a D configuration increases affinity. These studies led to the discovery of the peptide *cyclo*(RGDf[N–Me]V) (Cilengitide, EMD 121974), with a great affinity for the $\alpha_v\beta_3$ integrin.[15] A Phase III study of Cilengitide is being conducted in patients with glioblastoma, a very aggressive type of brain tumor.[5] Cilengitide is also in Phase II trials for the treatment of several other tumors.[5]

In the last years the use of 1,2,3-triazoles in peptide synthesis has increased due to the fact that triazole rings are amide bond isosters. Thus, they have been applied in the synthesis of polypseudopeptides, hydrogels, and peptidic nanotubes.[16] Since the discovery by Sharpless[17] of the copper catalysts for the Huisgen 1,3-dipolar azide–alkyne cycloaddition, this reaction has been used in the synthesis of 1,2,3-triazoles. The high yields obtained, the total regioselectivity, the mild reaction conditions, and the possibility to use water as solvent are some of the advantages of this reaction.[18] This reaction has also the advantage to be easily applied in peptide synthesis including solid-phase peptide synthesis since azide and alkyne units are easily incorporated into peptide sequences without protection.[19] The copper catalyzed Huisgen 1,3-dipolar cycloaddition can also be used as a valuable strategy for the synthesis of cyclic peptides.[18]

* Corresponding author. Tel.: +351 253604055; fax: +351 253604386; e-mail address: pmf@quimica.uminho.pt (P.M.T. Ferreira).

http://dx.doi.org/10.1016/j.tet.2014.06.121
0040-4020/

Taking into account the activity of *cyclo*(RGDf[N–Me]V) towards integrin $\alpha_v\beta_3$ and the advantages presented by the Huisgen 1,3-dipolar cycloaddition in the cyclization of peptides, it was decided to prepare two new cyclic peptides containing the RGDfV sequence and two triazolyl moieties. Molecular dynamics simulations and docking experiments were also performed in order to evaluate the potential affinity of the new peptides for the $\alpha_v\beta_3$ integrin, using *cyclo*(RGDf[N–Me]V) as a reference.

2. Results and discussion

The main synthetic objective of this work was to use a click chemistry approach to obtain cyclic RGD peptides having two 1,2,3-triazolyl moieties using a bis-alkynyl RGD peptide and bis-azides.

Initially the methodology was tested in the synthesis of two bis-amino acids, **3** and **4** (Scheme 1). Thus *tert*-butoxycarbonylglycine (Boc-Gly-OH), **1** was coupled with propargylamine giving the corresponding alkynylglycine, **2** in 96% yield. This compound was reacted with bis-azides yielding the corresponding bis-amino acids in good yields (Scheme 1). The bis-azides were prepared from the corresponding bis-boronic acids by treatment with sodium azide and copper(II) sulfate pentahydrate.[20] The bis-azides, namely the 1,4-diazidobenzene and the 2,7-diazido-9,9-dioctyl-9*H*-fluorene, were obtained in 67% and 87% yield, respectively.

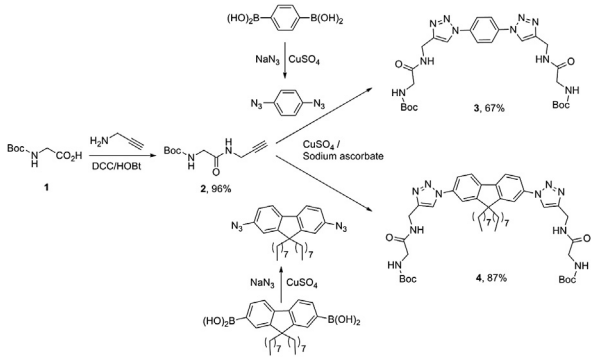

Scheme 1. Synthesis of bis-amino acids using a click chemistry approach by reacting an alkynylglycine derivative with two bis-azides.

In the ^{1}H NMR in DMSO of the bis-amino acids **3** and **4** it is possible to observe the signals corresponding to the two protons of the triazole ring at 8.68 ppm. Also, when comparing the chemical shifts of the aromatic protons of the bis-azides and of the bis-amino acids there is a downfield shift due to conjugation with the two triazole moieties. After testing this methodology with bis-amino acids it was decided to synthesize the cyclic RGD peptides **9** and **10** (Scheme 3). The RGDfV peptide *N*-conjugated with 5-hexynoic acid was synthesized by standard solid-phase peptide synthesis (SPPS) using a fluorenylmethoxycarbonyl (Fmoc) protocol and a 2-chlorotrityl chloride resin. For side-chain protection the 2,2,4,6,7-pentamethyl dihydrobenzofuran-5-sulfonyl (Pbf) group for arginine and the *tert*-butyl (^{t}Bu) group for aspartic acid were used. *N*-Fluorenylmethoxycarbonylvaline (*N*-Fmoc-L-Val-OH) was loaded into a 2-chlorotrityl chloride resin and the loading amount was determined to be 0.64 mol g^{-1}. The peptide was elongated by a N$^{\alpha}$-Fmoc strategy, and couplings were carried out with diisopropylcarbodiimide (DIC) and 1-hydroxybenzotriazole (HOBt) in dimethylformamide (DMF). The RGD peptide was coupled under solid-phase conditions with 5-hexynoic acid using the same methodology (Scheme 2). The peptide was cleaved from the resin with a mixture of 2,2,2-trifluoroethanol (TFE) and acetic acid (AcOH) in dichloromethane (DCM) to give peptide **5** in 49% yield. After cleavage from the resin peptide **5** was coupled with propargylamine using HOBt, *N*,*N*,*N*′,*N*′-tetramethyl-*O*-(1*H*-benzotriazol-1-yl)uronium hexafluorophosphate (HBTU), and *N*,*N*-diisopropylethylamine (DIPEA) giving peptide **6** in 92% yield (Scheme 2).

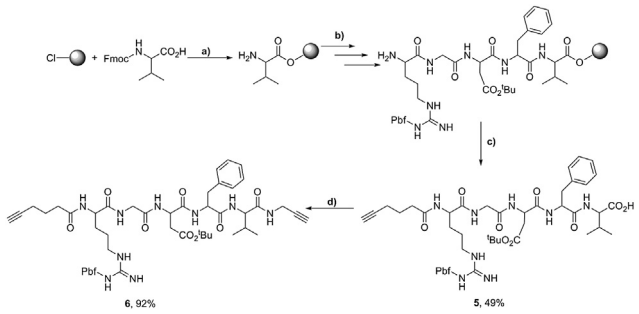

Scheme 2. Synthesis of the RGDfV peptide N,C-conjugated with alkyne moieties. a) (i) DIPEA, (ii) 20% piperidine/DMF; b) (i) Fmoc-aa-OH, HOBt, DIC, (ii) 20% piperidine/DMF; c) (i) 5-hexynoic acid, HOBt, DIC; (ii) AcOH/TFE; d) propargylamine, HOBt, HBTU, DIPEA.

Peptide **6** was reacted with the bis-azides, 1,4-diazidobenzene, and 2,7-diazido-9,9-dioctyl-9*H*-fluorene, to afford the corresponding cyclic RGD peptides in high yields (Scheme 3). However, better yields were obtained using the conditions described by Wu et al.[21] Peptides **7** and **8** were isolated in 82 and 97% yield, respectively. The new peptides **9** and **10** were obtained after deprotection (Scheme 3).

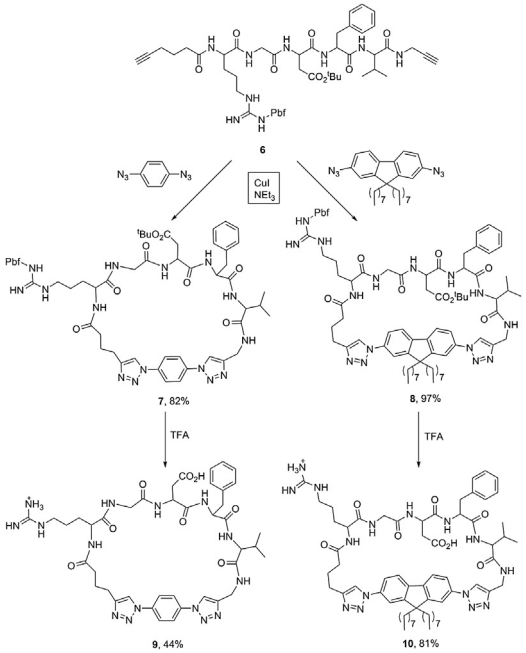

Scheme 3. Synthesis of the cyclic-RGDfV peptides **9** and **10**.

The interaction of peptides **9** and **10** with $\alpha_v\beta_3$ integrin was evaluated using molecular dynamic simulations and docking experiments. The AutoDock program was tested by re-docking of the X-ray structure of the binding mode of *cyclo*(RGDf[N–Me]V) (Cilengitide) with the extracellular fragment of the $\alpha_v\beta_3$ integrin. The root mean square deviation of the heavy atoms of the X-ray structure of Cilengitide and the re-docking of this peptide is 0.19 nm (Fig. 1). All the side chain groups of Cilengitide are docked

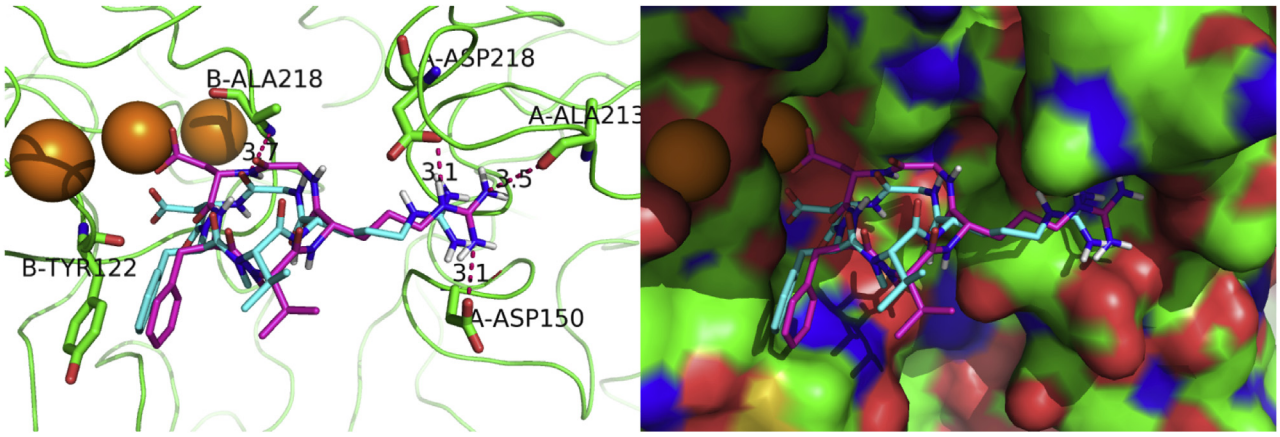

Fig. 1. Representation of the X-ray structure of the binding mode (carbons in cyan) and of the lowest binding energy conformation (carbons in pink, ΔG=−10.62 kcal/mol) of *cyclo*(RGDf[N−Me]V) (Cilengitide) in the $\alpha_v\beta_3$ integrin active site.

in the same binding pocket regions, establishing hydrogen bond interactions with Asp218, Ala213, Asp150, and Ala218, ionic interactions with the metal ion and hydrophobic interactions with Tyr122. Since the program was successful in reproducing the binding mode found experimentally, giving a binding free energy of ΔG=−10.62 kcal/mol (Fig. 1) it was decided to use it with the new cyclic peptides prepared. However, as the AutoDock program considers the backbone of cyclic peptides as being rigid, molecular dynamic simulations were carried out for peptides **9** and **10** to sample a large number of conformations with high probability of existing in an aqueous media. We selected 201 conformations from a 5 ns equilibrated MD simulation of each peptide (we sampled one conformation every 25 ps). The automated docking of these conformations gives a better sampling of the peptide conformational space. Figs. 2 and 3 show the molecular interactions of peptides **9** and **10** with the active center of the integrin.

The conformation of peptide **9** with the lowest binding energy and most populated cluster (ΔG=−15.13 kcal/mol) shows a docking pose in the active center of the integrin positioned between the two chains of the protein (Fig. 2, *top*). The binding mode differs from

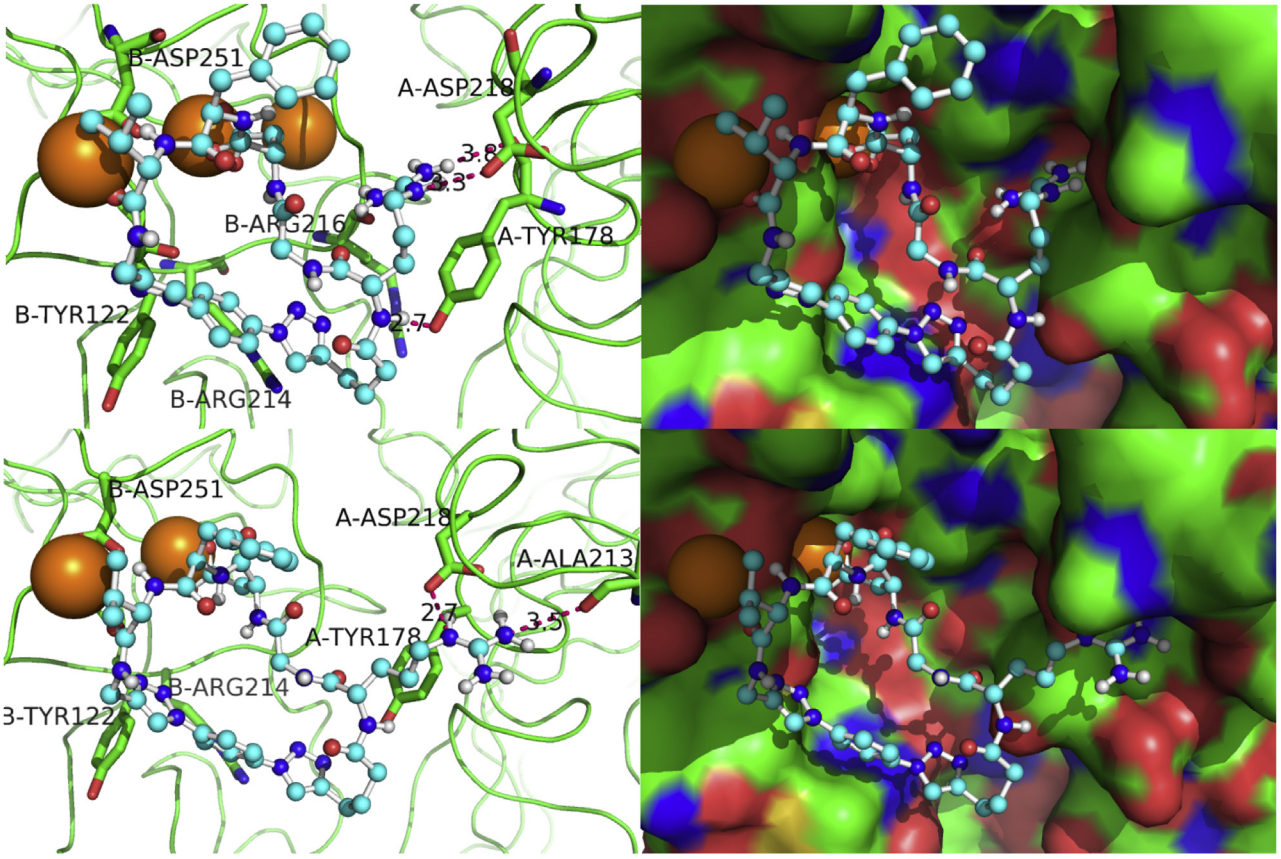

Fig. 2. Representation of the interactions between the two lowest binding energy conformations of peptide **9** and $\alpha_v\beta_3$ integrin (*Top*: ΔG=−15.13 kcal/mol, *Bottom*: ΔG=−13.63 kcal/mol).

that of *cyclo*(RGDf[N–Me]V), fitting the arginine side chain in a different pocket. This conformation shows three possible coordination bonds, one between the aspartic acid side chain and one Mn^{2+} ion, other between the same ion and the aspartic acid backbone, and the third between the carbonyl group of valine and another Mn^{2+} ion. The guanidium group of arginine is stabilized by salt bridges with the side chain of Asp218 and by the backbone of Arg216 and Tyr178. The amide bond between arginine and the linker of the peptide participates in a hydrogen bond with Tyr178 side chain. One of the triazole rings can participate in a salt bridge with Arg214. The phenyl group has an orientation that allows a T-shape interaction with Tyr122. This aromatic linker lies directly on the surface of the β-subunit of the protein. The amide proton of valine forms a hydrogen bond with Asp251 side chain. Phenylalanine inserts in a hydrophobic groove.

The conformation of peptide **9** with the binding free energy of ΔG=−13.63 kcal/mol (second best of peptide **9**) (Fig. 2, *bottom*) is similar to that of *cyclo*(RGDf[N–Me]V), as the arginine side chain inserts in the same groove. Salt bridges are formed with Asp218 side chain and Ala213. The amide bond between arginine and the spacer forms a salt bridge with the hydroxyl group of Tyr178 and the amide bond between valine and phenylalanine with Asp251 side chain. This conformation also shows coordination bonds with valine backbone and a metal ion and between aspartic acid side chain and another metal ion. The spacer lies on the surface of the integrin, establishing hydrophobic interactions, possibly in T-shape between one triazole ring and Tyr122, and dipole–dipole interactions between the other triazole ring and the side chain of Arg214 and Tyr166.

The docking experiments carried out with all conformations of peptide **10** gave similar results. The conformation with the lowest binding free energy and most populated cluster (ΔG=−17.56 kcal/mol) is represented in Fig. 3. The backbone of the peptide is inserted in the integrin in order to minimize the contact of the aromatic spacer with the solvent, but keeping important interactions with the protein. All the conformations show a coordination bond between the carboxylic group of aspartic acid with a metal ion, a salt bridge between the carbonyl group of aspartic acid or phenylalanine with Asn313 and a hydrogen bond of a triazole ring with the hydroxyl group of Tyr178. The phenylalanine side chain adopts an orientation inside the peptide backbone, parallel to the aromatic spacer, allowing hydrophobic π–π stacking. One of the alkyl chains of the spacer establishes hydrophobic interactions within a pocket of the integrin. As for the other alkyl chain of the spacer, it seems to flow on the solvent, adopting different orientations for each binding conformation. The arginine side chain can also establish salt bridges with four different regions with a negative partial charge on the surface of the integrin.

Both peptides **9** and **10** have shown theoretical binding energies much lower than that of the reference peptide used, *cyclo*(RGDf[N–Me]V) (Cilengitide). This suggests stronger interactions with the protein. It was expected an increase in hydrophobic interactions, however it was also possible to detect an increase in other types of interactions, such as hydrogen bridges and electrostatic interactions.

The spacer in peptide **9** seems to induce an alteration in the geometry of the RGDfV sequence. There are two new coordination bonds when comparing to Cilengitide and the Asp side chain is closer to the metal ion thus increasing the strength of this bond. The amide bond between valine and phenylalanine also establishes a salt bridge, which indicates that in the case peptide **9** methylation of valine nitrogen would be unfavorable. As for the spacer it seems that it contributes to the lower binding energy, as it lies perfectly on the integrin surface establishing hydrophobic interactions (T-shape) and possibly a salt bridge between one triazole ring and an arginine.

Peptide **10** fills completely the spaces of the active site of the integrin. The spacer seems to contribute to the low binding energy, increasing the hydrophobic interactions and creating a new salt bridge. As one of the alkyl chains does not seems to establish interactions with the integrin, the use of a similar spacer with a functional group in this chain would be a good option to link other agents. The new orientation of the phenylalanine side chain increases the stability of the peptide and binding in the proper conformation.

3. Conclusions

The Huisgen 1,3-dipolar azide–alkyne cycloadditions carried out in this work proved to be an excellent methodology for the synthesis of bis-amino acids and for the cyclization of peptides. In the case of bis-amino acids the best yields were obtained in the presence of a copper(II) salt and a reducing agent, which generates the reactive Cu(I) in situ, while the best result in the cyclization of peptide **6** was obtained using a copper(I) species.

The dynamic molecular simulations and docking studies showed that both peptides, in particular peptide **10**, have a higher binding free energy to integrin $\alpha_v\beta_3$ than Cilengitide, which suggest a higher affinity to this integrin. Thus, peptides **9** and **10** represent two new potential integrin $\alpha_v\beta_3$ antagonists. This affinity will be further studied by *in vitro* integrin-binding assays.

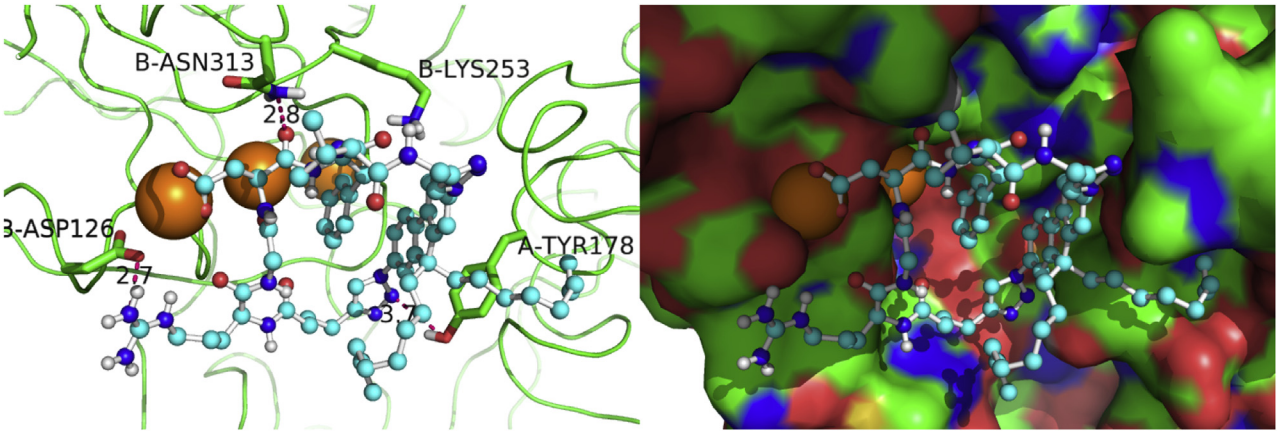

Fig. 3. Representation of the interactions between the lowest binding energy conformation of peptide **10** and $\alpha_v\beta_3$ integrin (ΔG=−17.56 kcal/mol).

4. Experimental section

4.1. General methods

Melting points (mp, in °C) were determined in a Gallenkamp apparatus and are uncorrected. ^{1}H and ^{13}C NMR spectra were recorded on a Bruker Avance II^{+} at 400 and 100.6 MHz, respectively. $^{1}H-^{1}H$ spin–spin decoupling, DEPT θ 45°, HMQC, and HMBC were used. Chemical shifts are given in parts per million (ppm) and coupling constants in hertz (Hz). The solvents used in the NMR data were chloroform-d ($CDCl_3$) or dimethylsulfoxide-d_6 (DMSO). High resolution mass spectrometry (HRMS) data were recorded by the mass spectrometry service of the University of Vigo, Spain. Elemental analysis was performed on an LECO CHNS 932 elemental analyzer. The infrared (IR) spectra were recorded in a Bomen MB 104 spectrophotometer. The samples were prepared in Nujol, using sodium chloride cells. The ultraviolet/visible (UV–vis) spectra were recorded in a Shimadzu UV-2501PC equipment. Some reactions were monitored by thin layer chromatography (TLC), using precoated TLC-sheets Alugram Xtra SIL G/UV254. The sheets were revealed in UV light (254 nm). DCM was dried over calcium chloride ($CaCl_2$) and calcium hydride (CaH_2) and then distilled and stored under molecular sieves. Petroleum ether refers to the boiling range 40–60 °C. In SPPS was used the resin 2-chlorotrytil chloride (100–200 mesh) 1% DVB, with a loading capacity of 1 mmol/g. The 2,4,6-trinitrobenzenesulfonic acid (TNBS) test[22] was used to evaluate the deprotection/coupling cycles.

4.1.1. Cyclopeptides force field parameters. The linkers in each cyclopeptide were parameterized. The linkers were constructed using the molecular visualization program PyMOL. Geometry optimization of the all atom model of each linker was performed at the B3LYP level with GAUSSIAN03, using the 6-31G(d) basis set for organic atoms (C, H, N, and O). Partial atomic charges were obtained using the RESP fitting method, based on electrostatic potentials calculated at the Hartree Fock level with the 6-31G(d) basis set in GAMESS. A two-step RESP fitting procedure was used in order to build a united atom model in agreement with the Amber11 force field. The parameterization of the peptides was done using the Amber99SB force field. Missing bonded parameters were taken from the general Amber force field (GAFF),[23] as usually done in Amber when new molecules need to be parameterized. Both force fields are present in the Amber11 distribution. Initially, the charges of the abstracted hydrogens (a process used in GROMOS to collapse a hydrogen to its attached aliphatic carbon) were given zero partial charge and the charges of the oxygen atoms were equalized. The charges of the atoms in the linkers that corresponded to amide bonds in the cyclopeptides were corrected, using the parameters in the force field Amber11, and the charges were calculated again. Then the optimized geometry of each linker was used to build the cyclopeptides in the molecular visualization program PyMOL.

4.1.2. Simulation setup. Molecular mechanics/molecular dynamics (MM/MD) simulations were performed with the GROMACS 4.5.4 package[24] using the Amber99SB force field.[25] Each peptide was hydrated in a pre-equilibrated dodecahedron box of SPC waters at 300 K. The system size was chosen according to the minimum image convention taking into account a cut off of 1 Å. A system with zero net charge was obtained by replacement of solvent molecules by equivalent number of Na^{+} atoms. The initial systems were energy minimized for 100,000 steps using the steepest descent method with all protein heavy atoms harmonically restrained using a force constant of 10^6 kJ/mol nm^2. Subsequently, 100,000 steps of energy minimization with positional restrains applied to the αC protein atoms were carried out followed by 100,000 steps of unrestrained full system energy minimization. The cyclopeptides were initialized in the canonical ensemble (NVT) for 200 ps with all protein heavy atoms harmonically restrained using a force constant of 10^6 kJ/mol nm^2, followed by 200 ps with positional restrains applied to the protein Cα atoms. The simulation was continued for 10 ns in the isothermal–isobaric ensemble (NPT) to ensure the full equilibration of all system properties. Pressure control was implemented using the Berendsen barostat[26] with a reference pressure of 1 atm, 0.5 ps relaxation time, and isothermal compressibility of 4.5×10^{-5} bar^{-1}. Temperature control was set using the Berendsen thermostat[26] at 298 K. The peptides and the solvent molecules were grouped in separate heat baths with temperature coupling constants of 0.1 ps both in the initialization and in the equilibration phases. The conformations were recorded at a frequency of 1/ps, leading to a trajectory file containing 10,000 frames. Conformations were taken from the last 5 ns (5000 frames) of the simulation run. We extracted a total of 201 conformations using a 25 ps interval.

4.1.3. Protein set-up. The structure of the extracellular fragment of the $\alpha_v\beta_3$ integrin[27] is deposited in the Protein Data Bank (PDB) with code 1L5G. The protonation states of the acidic and basic residues were set to their standard states found in aqueous solution at pH 7. All acidic residues of the protein were fully deprotonated, and all basic residues were fully protonated. The *N*-termini were protonated and the *C*-termini were deprotonated.

4.1.4. Docking. Structural integrin–cyclopeptide complexes and theoretical binding free energy of the X-ray structure of the binding mode of peptide *cyclo*(RGDf[N–Me]V)[27] and of the conformations of peptides **9** and **10** towards the active site of integrin $\alpha_v\beta_3$ were done with computational docking methodologies, using AUTODOCK4.[28] In the docking calculations, all possible torsions in the side chains of the cyclopeptides were set flexible, except the guanidine group in arginine. The torsions in the main chain of the cyclopeptides were constrained. The protonation states of the acidic and basic residues in the cyclopeptides were set to their standard state found in aqueous solution at pH 7. The conformations obtained from the MD simulations of each cyclopeptide were used. The grid for probe-target energy calculations was placed with its center at the integrin-binding site (x=19.50 Å, y=43.96 Å, z=44.15 Å). The docking grid size was 40×40×40 grid points with 0.375 Å spacing. For each cyclopeptide, 150 runs using the Lamarckian genetic algorithm with 150 individuals in each population were carried out. The maximum number of generations was set to 27×10^3 and the maximum number of energy evaluations to 25×10^5. The resulting docking solutions were clustered using AUTODOCK with a structural root mean square deviation cut-off of 1 Å. The structural complex of lowest-energy ligand–protein complexes was analyzed.

4.2. Synthesis

4.2.1. Synthesis of 1,4-diazidobenzene. To a solution of sodium azide (5.00 mmol; 0.32 g) and copper(II) sulfate pentahydrate (0.40 mmol; 99.80 mg) in methanol (5 mL), 1,4-phenylene diboronic acid (2.00 mmol; 0.33 g) was added. The reaction mixture was left stirring at room temperature for 40 h. The solvent was removed under reduced pressure and the residue treated with petroleum ether. The solvent was removed to give the 1,4-diazidobenzene (0.21 g; 67%) as an orange solid. Mp 79.0–82.0 °C (from petroleum ether). IR (Nujol): ν=2954 (C–H), 2924 (C–H), 2854 (C–H), 2107 (N_3) cm^{-1}. ^{1}H NMR (400 MHz, $CDCl_3$): δ=7.02 (4H, s, ArH) ppm. ^{13}C NMR (100.6 MHz, $CDCl_3$): δ=120.34 (CH), 136.67 (C) ppm. $C_6H_4N_6$ (160.14): calcd C 45.00, H 2.52, N 52.48; found C 45.12, H 2.70, N 52.25.

4.2.2. Synthesis of 2,7-diazido-9,9-dioctyl-9H-fluorene. To a solution of sodium azide (2.50 mmol; 0.16 g) and copper(II) sulfate

pentahydrate (0.20 mmol; 0.05 g) in methanol (3 mL), 9,9-dioctyl-9*H*-fluorene-2,7-diyldiboronic acid (1.00 mmol; 0.48 g) was added. The reaction mixture was left stirring at room temperature for 30 h. The solvent was removed under reduced pressure and the residue treated with petroleum ether. The solvent was removed to give the 2,7-diazido-9,9-dioctyl-9*H*-fluorene (0.41 g; 87%) as a green solid. Mp 64.0–66.0 °C (from petroleum ether). IR (Nujol): ν=2954 (C–H), 2925 (C–H), 2854 (C–H), 2103 (N_3) cm^{-1}. ^1H NMR (400 MHz, $CDCl_3$): δ=0.57–0.61 (4H, m, CH_2), 0.82–0.89 (6H, m, 2×CH_3), 1.05–1.06 (8H, m, CH_2), 1.11–1.15 (8H, m, CH_2), 1.20–1.23 (4H, m, CH_2), 1.91–1.96 (4H, m, CH_2), 6.96 (2H, d, *J*=2.0 Hz, 2×ArH), 7.01 (2H, dd, *J*=2.0 and 8.0 Hz, 2×ArH), 7.61 (2H, d, *J*=8.0 Hz, 2×ArH) ppm. ^{13}C NMR (100.6 MHz, $CDCl_3$): δ=14.03 (CH_3), 22.56 (CH_2), 23.60 (CH_2), 29.16 (CH_2), 29.86 (CH_2), 31.74 (CH_2), 40.35 (CH_2), 55.43 (C), 113.56 (2×CH), 117.85 (2×CH), 120.52 (2×CH), 137.58 (2×C), 138.71 (2×C), 152.56 (2×C) ppm.

4.2.3. Synthesis of tert-butyl 2-oxo-2-(prop-2-ynylamino)ethylcarbamate ***2***. To a solution of Boc-Gly-OH (10 mmol; 1.75 g) in acetonitrile (10 mL), HOBt (10 mmol; 1.35 g), *N*,*N*′-dicyclohexylcarbodiimide (DCC) (10 mmol; 2.06 g), propargylamine (10 mmol; 0.69 mL), and triethylamine (10 mmol; 1.40 mL) were added. The reaction mixture was left stirring at room temperature overnight, filtered, and the solvent was removed under reduced pressure. The residue was dissolved in ethyl acetate (100 mL), washed with aqueous solutions of $KHSO_4$ 1 M (3×50 mL), $NaHCO_3$ 1 M (3×50 mL), and brine (3×50 mL) and dried with anhydrous $MgSO_4$. The solvent was removed under reduced pressure to give compound **2** (2.03 g, 96%) as a white solid. Mp 100.0–101.5 °C (from ethyl acetate/petroleum ether). ^1H NMR (400 MHz, $CDCl_3$): δ=1.45 (9H, s, 3×CH_3), 2.23 (1H, t, *J*=2.4 Hz, CH), 3.82 (2H, d, *J*=5.6 Hz, αCH_2), 4.06 (2H, dd, *J*=2.4 and 5.6 Hz, CH_2), 5.29 (1H, br s, NH), 6.51 (1H, br s, NH) ppm. ^{13}C NMR (100.6 MHz, $CDCl_3$): δ=28.26 (CH_3), 29.03 (CH_2), 44.26 (αCH_2), 71.63 (CH), 79.19 (*C*≡CH), 80.42 (*C*(CH_3)$_3$), 156.09 (C=O), 169.25 (C=O) ppm. $C_{10}H_{16}N_2O_3$ (212.25): calcd C 56.59, H 7.69, H 13.20; found C 57.36, H 7.76, N 12.57.

4.2.4. Synthesis of tert-butyl 2,2′-(1,1′-(1,4-phenylene)bis(1H-1,2,3-triazole-4,1-diyl))bis(methylene)bis(azanediyl)bis(2-oxoethane-2,1-diyl)dicarbamate ***3***. To a solution of compound **2** (0.55 mmol; 0.12 g) in methanol (1 mL) and water (1 mL), 1,4-diazidobenzene (0.25 mmol; 0.04 g), copper(II) sulfate (0.05 mmol; 0.01 g), and sodium ascorbate (0.25 mmol; 0.05 g) were added. The reaction mixture was left stirring at room temperature for 20 h. The solvent was removed under reduced pressure and the residue treated with ethyl acetate. The solid formed was filtered giving compound **3** (0.13 g; 92%) as a white solid. ^1H NMR (400 MHz, DMSO): δ=1.37 (18H, s, 6×CH_3), 3.57 (4H, d, *J*=6.0 Hz, αCH_2), 4.41 (4H, d, *J*=5.4 Hz, CH_2), 6.97 (2H, t, *J*=5.4 Hz, NH), 8.10 (4H, s, ArH), 8.41 (2H, t, *J*=6.0 Hz, NH), 8.68 (2H, s, CH) ppm. ^{13}C NMR (100.6 MHz, DMSO): δ=28.19 (6×CH_3), 34.17 (CH_2), 43.29 (αCH_2), 78.09 (*C*(CH_3)$_3$), 121.20 (4×CH), 121.24 (CH), 136.18 (C), 146.49 (C), 155.87 (C=O), 169.53 (C=O) ppm. HRMS (M+H): calcd $C_{26}H_{37}N_{10}O_6$ 585.28921; found 585.28909.

4.2.5. Synthesis tert-butyl 2,2′-[1,1′-(9,9-octyl-9H-fluorene-2,7-diyl) bis(1H-1,2,3-triazole-4,1-diyl)]bis(methylene)bis(azanediyl)bis(2-oxoethane-2,1-diyl)dicarbamate ***4***. To a solution of compound **2** (0.55 mmol; 0.12 g) in methanol (1 mL) and water (1 mL), 2,7-diazido-9,9-octyl-9*H*-fluorene (0.25 mmol; 0.12 g), copper(II) sulfate (0.05 mmol; 0.01 g), and sodium ascorbate (0.25 mmol; 0.05 g) were added. The reaction mixture was left stirring at room temperature for 24 h. The solid formed in the reaction mixture was filtered and washed with petroleum ether, giving compound **4** (0.06 g, 25%) as a light green solid. Mp degrades above 180 °C. ^1H NMR (400 MHz, DMSO): δ=0.44–0.58 (4H, m, 2×CH_2), 0.71 (6H, t, *J*=6.9 Hz, 2×CH_3), 0.92–1.24 (20H, m, 10×CH_2), 1.37 (18H, s, 6×CH_3), 2.08–2.18 (4H, m, 2×CH_2), 3.56 (4H, d, *J*=6.0 Hz, CH_2 Gly), 4.41 (4H, d, *J*=5.1 Hz, NH*C*H_2), 6.99 (2H, t, *J*=6.0 Hz, NH), 7.89 (2H, d, *J*=7.8 Hz, 2×ArH), 8.02 (2H, s, 2×ArH), 8.08 (2H, d, *J*=8.1 Hz, 2×ArH), 8.40 (2H, t, *J*=5.1 Hz, NH), 8.68 (2H, s, CH) ppm. ^{13}C NMR (100.6 MHz, DMSO): δ=13.77 (2×CH_3), 21.91 (CH_2), 23.28 (CH_2), 24.43 (CH_2), 25.29 (CH_2), 28.15 (6×CH_3), 28.42 (CH_2), 31.01 (αCH_2), 33.31 (CH_2), 34.16 (NH*C*H_2), 43.29 (CH_2 Gly), 55.76 (C), 78.00 (*C*(CH_3)$_3$), 114.57 (2×CH), 119.00 (2×CH), 121.22 (CH), 121.49 (2×CH), 136.14 (2×C), 139.66 (2×C), 152.31 (2×C), 155.84 (C), 156.60 (C=O), 169.45 (C=O) ppm. $C_{49}H_{72}N_{10}O_6$ (897.16): calcd C 65.60, H 8.09, N 15.61; found C 65.68, H 8.25, N 15.00.

4.2.6. Synthesis of peptide ***5***. To a solution of Fmoc-L-Val-OH (1.20 mmol, 0.41 g) in dry DCM (10 mL), DIPEA (4.80 mmol, 0.83 mL), and resin (1.00 g) were added. The mixture was left stirring at room temperature for 2 h. The solvent was removed and the resin was washed with a mixture of DCM/MeOH/DIPEA (17:2:1, 3×10 mL), DCM (3×10 mL), DMF (3×10 mL), and DCM (3×10 mL). The resin was left drying under reduced pressure overnight. A solution of 20% of piperidine in DMF (50 mL) was prepared. This solution (10 mL) was added to a sample of the resin loaded with the amino acid (3.33 mg) and strongly stirred. The absorbance (Abs) of this solution was measured at 290 nm. The loading of the resin was 0.64 mmol/g. After washing the resin with DMF (2×10 mL), a solution of 20% of piperidine in DMF (10 mL) was added. The mixture was left stirring at room temperature for 2 h. The solvent was filtered and the resin was washed successively with DMF (2×10 mL), 2-propanol (2×10 mL), DMF (2×10 mL), and 2-propanol (2×10 mL). The TNBS test was used to verify the cleavage of the Fmoc group. Fmoc-D-Phe-OH (1.28 mmol, 0.54 g), HOBt (1.28 mmol, 0.17 g), and DIC (1.28 mmol, 0.20 mL) were dissolved in DMF (10 mL) and the solution was added to the resin. The mixture was left stirring at room temperature overnight. The solvent was removed and the resin was washed successively with DMF (3×10 mL) and DCM (3×10 mL). The coupling was verified by the TNBS test. The cleavage and coupling cycles were repeated for Fmoc-L-Asp(O^{t}Bu)-OH, Fmoc-Gly-OH, Fmoc-L-Arg(Pbf)-OH, and 5-hexynoic acid. Cleavage of the peptide from the resin was carried out using a mixture of AcOH/TFE/DCM (1:1:3, 20 mL). The mixture was filtered to remove the resin and the solvent evaporated under reduced pressure. Peptide **5** (0.33 g, 49%) was obtained as a white solid from diethyl ether. ^1H NMR (400 MHz, DMSO): δ=0.80 (6H, d, *J*=6.8 Hz, CH_3 Val), 1.32 (9H, s, 3×CH_3), 1.37–1.55 (3H, m, γCH_2 Arg, βCH_2 Arg), 1.40 (6H, s, 2-CH_3 Pbf), 1.63 (3H, m, βCH_2 Arg, CH_2C*H*$_2$$CH_2$), 1.97–2.02 (1H, m, βCH Val), 1.99 (3H, s, CH_3 Pbf), 2.12 (2H, dt, *J*=2.4 and 7.2 Hz, CH≡CC*H*$_2$), 2.21 (2H, t, *J*=7.4 Hz, C*H*$_2$C=O), 2.20–2.26 (1H, m, βCH_2 Asp), 2.37–2.44 (1H, m, βCH_2 Asp), 2.40 (3H, s, CH_3 Pbf), 2.46 (3H, s, CH_3 Pbf), 2.75 (1H, t, *J*=2.4 Hz, C*H*≡CCH$_2$), 2.77 (1H, d, *J*=3.6 Hz, βCH_2 Phe), 2.95 (2H, s, 3-CH_2 Pbf), 2.96–2.98 (1H, m, βCH_2 Phe), 2.98–3.02 (2H, m, δCH_2 Arg), 3.61–3.64 (2H, m, αCH_2 Gly), 4.11 (1H, dd, *J*=6.0 and 8.4 Hz, αCH Val), 4.20 (1H, dd, *J*=7.6 and 13.2 Hz, αCH Arg), 4.54 (1H, dd, *J*=8.4 and 13.2 Hz, αCH Asp), 4.63 (1H, dd, *J*=4.4 and 9.2 Hz, αCH Phe), 6.50 (2H, br s, 2×NH), 6.91 (1H, br s, NH), 7.14–7.17 (1H, m, ArH Phe), 7.19–7.24 (4H, m, ArH Phe), 8.04–8.06 (3H, m, NH Asp, NH Phe, NH Val), 8.12 (1H, d, *J*=7.2 Hz, NH Arg), 8.23 (1H, br s, NH Gly), 12.40 (1H, br s, CO_2H) ppm. ^{13}C NMR (100 MHz, DMSO): δ=12.26 (CH_3 Pbf), 17.41 (CH≡C*C*H$_2$), 17.58 (CH_3 Pbf), 17.91 (CH_3 Val), 18.93 (CH_3 Pbf), 19.11 (CH_3 Val), 24.08 (CH_2*C*H$_2$$CH_2$), 25.44 (γ$CH_2$ Arg), 27.61 (3×CH_3), 28.29 (2-CH_3 Pbf), 28.98 (βCH_2 Arg), 30.13 (βCH Val), 33.94 (*C*H$_2$C=O), 37.53 (βCH_2 Asp), 38.14 (βCH_2 Phe), 41.99 (CH_2 Gly), 42.46 (3-CH_2 Pbf), 43.74 (δCH_2 Arg), 49.29 (αCH Asp), 52.55 (αCH Arg), 54.03 (αCH Phe), 57.33 (αCH Val), 71.44 (*C*H≡CCH$_2$), 80.06 (*C*(CH_3)$_3$), 84.04 (CH≡**C**CH$_2$), 86.27 (2-C Pbf), 116.23 (C Pbf), 124.30 (C Pbf), 126.22 (CH Phe), 127.94 (CH Phe), 129.21 (CH Phe), 131.41 (C Pbf), 134.20 (C

Pbf), 137.25 (C Pbf), 137.66 (C Phe), 156.10 (C=N Arg), 157.42 (C Pbf), 168.50 (C=O Gly), 169.07 (βC=O Asp), 169.92 (C=O Asp), 170.80 (C=O Phe), 172.00 (CH_2C=O), 172.27 (C=O Arg), 173.07 (CO_2H) ppm. HRMS [M+H] (EI): calcd $C_{49}H_{71}N_8O_{12}S$ 995.49067; found 995.48985.

4.2.7. Synthesis of peptide ***6****.* Peptide **5** (0.10 mmol, 0.11 g) was dissolved in DMF (5 mL) and the mixture cooled in an ice bath. HOBt (0.10 mmol, 0.01 g), HBTU (0.10 mmol, 0.04 g), and propargylamine (0.10 mmol, 0.01 mL) were added, waiting 5 min between each addition. DIPEA (0.21 mmol, 0.04 mL) was added and the mixture was left stirring at room temperature for 2 days. The DMF was removed under reduced pressure. Peptide **6** was precipitated from water (0.10 g, 92%) as a white solid. ^{1}H NMR (400 MHz, DMSO): δ=0.75 (6H, d, J=6.4 Hz, CH_3 Val), 1.32 (9H, s, 3×CH_3), 1.39–1.41 (2H, m, γCH_2 Arg), 1.40 (6H, s, 2-CH_3 Pbf), 1.47–1.62 (2H, m, βCH_2 Arg), 1.64 (2H, m, $CH_2CH_2CH_2$), 1.91 (1H, m, βCH Val), 1.99 (3H, s, CH_3 Pbf), 2.12 (2H, dt, J=2.4 and 7.2 Hz, CH≡CCH_2), 2.21 (2H, t, J=7.6 Hz, CH_2C=O), 2.21–2.22 (1H, m, βCH_2 Asp), 2.37 (1H, s, βCH_2 Asp), 2.41 (3H, s, CH_3 Pbf), 2.46 (3H, s, CH_3 Pbf), 2.75 (1H, t, J=2.4 Hz, CH≡CCH_2), 2.78 (1H, d, J=9.6 Hz, βCH Phe), 2.95 (2H, s, 3-CH_2 Pbf), 2.97 (1H, d, J=8.8 Hz, βCH Phe), 2.98–3.02 (2H, m, δCH_2 Arg), 3.06 (1H, t, J=2.4 Hz, CH≡CCH_2NH), 3.68 (2H, t, J=6.8 Hz, CH_2 Gly), 3.79 (2H, ddq, J=2.4, 5.6, and 17.6 Hz, CH≡CCH_2NH), 4.09 (1H, dd, J=7.4 and 8.6 Hz, αCH Val), 4.20 (1H, q, J=7.6 Hz, αCH Arg), 4.53–4.57 (1H, m, αCH Asp), 4.59–4.63 (1H, m, αCH Phe), 6.39 (1H, br s, NH), 6.66 (2H, br s, 2×NH), 7.13–7.17 (1H, m, ArH Phe), 7.19–7.23 (4H, m, ArH Phe), 8.02 (1H, d, J=8.8 Hz, NH Asp), 8.06 (3H, d, J=9.2 Hz, αNH Arg, NH Phe, NH Val), 8.17 (1H, t, J=5.2 Hz, NH Gly), 8.45 (1H, t, J=5.2 Hz, CH≡CCH_2NH) ppm. ^{13}C NMR (100 MHz, DMSO): δ=12.25 (CH_3 Pbf), 17.40 (CH≡CCH_2), 17.56 (CH_3 Pbf), 18.09 (CH_3 Val), 18.91 (CH_3 Pbf), 18.99 (CH_3 Val), 24.07 ($CH_2CH_2CH_2$), 25.45 (γCH_2 Arg), 27.60 (3×CH_3), 27.76 (CH≡CCH_2NH), 28.28 (2-CH_3 Pbf), 29.06 (βCH_2 Arg), 30.58 (βCH Val), 33.90 (CH_2C=O), 37.62 (βCH_2 Asp), 38.02 (βCH_2 Phe), 40.29 (δCH_2 Arg), 41.90 (CH_2 Gly), 42.45 (3-CH_2 Pbf), 49.24 (αCH Asp), 52.53 (αCH Arg), 54.13 (αCH Phe), 57.50 (αCH Val), 71.42 (CH≡CCH_2), 72.85 (CH≡CCH_2NH), 80.06 (C(CH_3)$_3$), 80.88 (CH≡CCH_2NH), 84.03 (CH≡CCH_2), 86.27 (2-C Pbf), 116.23 (C Pbf), 124.29 (C Pbf), 126.22 (CH Phe), 127.92 (CH Phe), 129.22 (CH Phe), 131.40 (C Pbf), 134.16 (C Pbf), 137.24 (C Pbf), 137.52 (C Phe), 156.01 (C=N), 157.42 (C Pbf), 168.46 (C=O Gly), 169.01 (βC=O Asp), 170.01 (C=O Asp), 170.69 (C=O Val), 170.71 (C=O Phe), 172.01 (CH_2C=O), 172.14 (C=O Arg) ppm. HRMS [M+H] (EI): calcd $C_{52}H_{74}N_9O_{11}S$ 1032.52230; found 1032.52280.

4.2.8. Synthesis of peptide ***7****.* To a solution of peptide **6** (0.05 mmol, 0.05 g) in DMF (2 mL), 1,4-diazidobenzene (0.05 mmol, 7.40 mg), copper(I) iodide (0.90 μmol, 0.20 mg), and triethylamine (0.10 mmol, 0.01 mL) were added and the mixture was left stirring at room temperature. The reaction was followed by TLC (chloroform/methanol, 9:1). After 84 h the solvent was removed and peptide **7** was precipitated from water (0.04 g; 82%). ^{1}H NMR (400 MHz, DMSO): δ=0.74 (6H, br s, CH_3 Val), 1.31 (9H, s, 3×CH_3), 1.33–1.40 (2H, m, γCH_2 Arg), 1.40 (6H, s, 2-CH_3 Pbf), 1.40–1.52 (1H, m, βCH_2 Arg), 1.58–1.65 (3H, m, βCH_2 Arg, $COCH_2CH_2$), 1.90–1.96 (1H, m, βCH Val), 1.98 (3H, s, CH_3 Pbf), 2.11–2.13 (2H, m, CH_2CH_2-triazole), 2.18–2.26 (3H, m, βCH_2 Asp, $COCH_2CH_2$), 2.39–2.45 (1H, m, βCH_2 Asp), 2.40 (3H, s, CH_3 Pbf), 2.45 (3H, s, CH_3 Pbf), 2.75–2.79 (1H, m, βCH_2 Phe), 2.93 (2H, s, 3-CH_2 Pbf), 2.93–3.00 (1H, m, βCH_2 Phe), 2.98–3.02 (2H, m, δCH_2 Arg), 3.67–3.72 (2H, m, CH_2 Gly), 4.13 (1H, dd, J=6.0 and 14.4 Hz, αCH Val), 4.19–4.21 (1H, m, αCH Arg), 4.38–4.46 (2H, m, NHCH_2), 4.50–4.58 (1H, m, αCH Asp), 4.58–4.65 (1H, m, αCH Phe), 6.39 (1H, br s, NH), 6.67 (2H, br s, 2×NH), 7.13–7.17 (1H, m, ArH Phe), 7.21–7.22 (4H, m, ArH Phe), 7.29 (1H, s, CH triazole), 7.88 (1H, s, CH triazole), 8.07–8.12 (8H, m, 4×NH, ArH), 8.19 (1H, br s, NH Gly), 8.54–8.55 (1H, m, NHCH_2) ppm. ^{13}C NMR (100 MHz, DMSO): δ=12.24 (CH_3 Pbf), 17.41 (CH_2CH_2), 17.57 (CH_3 Pbf), 18.92 (CH_3 Pbf), 18.02 (CH_3 Val), 19.11 (CH_3 Val), 24.07 ($COCH_2CH_2$), 25.48 (γCH_2 Arg), 27.57 or 27.59 (3×CH_3), 28.27 (2-CH_3 Pbf), 29.05 (βCH_2 Arg), 30.33 (βCH Val), 33.91 ($COCH_2CH_2$), 34.07 (NHCH_2), 37.58 (βCH_2 Asp), 37.93 (βCH_2 Phe), 40.18 (δCH_2 Arg), 41.93 (CH_2 Gly), 42.44 (3-CH_2 Pbf), 49.32 (αCH Asp), 52.26 (αCH Arg), 54.25 (αCH Phe), 57.75 (αCH Val), 80.09 (C(CH_3)$_3$), 86.27 (2-C Pbf), 116.22 (C Pbf), 120.39 (CH), 121.16 (CH), 121.16 (CH), 124.29 (C Pbf), 126.22 (CH Phe), 127.94 (CH Phe), 129.21 (CH Phe), 131.41 (C Pbf), 134.10 (C Pbf), 136.13 (C), 137.25 (C Pbf), 137.51 (C Phe), 145.93 (C), 147.66 (C), 156.02 (C=N), 157.42 (C Pbf), 168.54 (C=O), 169.03 (C=O), 170.12 (C=O), 170.87 (C=O), 170.89 (C=O), 172.06 (C=O), 172.11 (C=O) ppm. HRMS [M+H] (EI): calcd $C_{58}H_{78}N_{15}O_{11}S$ 1192.57205; found 1192.57320.

4.2.9. Synthesis of peptide ***8****.* To a solution of peptide **6** (0.10 mmol, 0.10 g) in DMF (1 mL), 2,7-diazido-9,9-dioctyl-9H-fluorene (0.15 mmol, 68.70 mg), copper(I) iodide (4.00 μmol, 0.80 mg), and triethylamine (0.29 mmol, 0.04 mL) were added. The mixture was left stirring at room temperature. The reaction was followed by ^{1}H NMR. After 72 h the solvent was removed and a mixture of peptide **8** and copper was precipitated from water. The solid was washed with an aqueous solution of ethylenediamine tetraacetic acid (EDTA) 0.1 M, giving peptide **8** (0.14 g, 97%) as a light brown solid. ^{1}H NMR (400 MHz, DMSO, 70 °C): δ=0.60 (4H, br s, 2×CH_2), 0.78–0.81 (12H, m, 2×CH_3 Val, 2×CH_3), 1.01–1.24 (18H, m, 9×CH_2), 1.32 (9H, s, 3×CH_3), 1.38–1.50 (4H, m, CH_2 Arg, CH_2 Arg), 1.60 (3H, br s, 2×CH_3 Pbf), 1.95–1.99 (2H, m, CH_2), 2.08 (8H, br s, βCH Val, CH_3 Pbf, 2×CH_2), 2.25–2.42 (4H, m, CH_2 Asp, CH_2), 2.43 (3H, s, CH_3 Pbf), 2.49 (3H, br s, CH_3 Pbf), 2.74 (4H, br s, 2×CH_2), 2.89–2.92 (6H, m, CH_2 Phe, CH_2 Arg, CH_2 Pbf), 3.74 (2H, br s, CH_2 Gly), 4–17 (1H, br s, αCH Val), 4.28 (1H, br s, αCH Arg), 4.45 (2H, br s, CH_2), 4.57(2H, br s, αCH Asp, αCH Phe), 6.43 (1H, br s, NH), 6.62 (1H, br s, NH), 7.06–7.08 (2H, m, ArH), 7.14–7.20 (7H, m, ArH), 7.75–7.95 (8H, m, 2×ArH, 4×NH), 8.29 (1H, br s, NH), 8.49–8.57 (2H, m, 2×NH) ppm. ^{13}C NMR (100 MHz, DMSO, 70 °C): δ=11.71 (CH_3), 13.27 (2×CH_3), 17.01 (CH_3), 18.32 (CH_3), 18.69 (2×CH_3), 21.45 (CH_2), 22.81 (CH_2), 24.43 (CH_2), 24.54 (CH_2), 25.16 (CH_2), 27.32 (3×CH_3), 27.84 (2×CH_3), 28.58 (CH_2), 28.69 (CH_2), 28.78 (CH_2), 30.15 (CH), 30.63 (CH_2), 33.93 (CH_2), 34.36 (CH_2), 37.12 (CH_2), 37.38 (CH_2), 38.57 (CH_2), 39.85 (CH_2), 41.90 (CH_2), 42.27 (CH_2), 45.97 (CH_2), 49.37 (CH), 52.35 (CH), 54.19 (CH), 54.94 (C), 57.72 (CH), 79.79 (C(CH_3)$_3$), 85.80 (C), 113.52 (CH), 116.0 (C), 117.71 (CH), 119.79 (CH), 120.59 (CH), 120.84 (CH), 124.0 (C), 125.80 (CH), 127.57 (CH), 128.74 (CH), 131.17 (C), 134.16 (C), 136.82 (C), 137.00 (C), 137.95 (C), 139.28 (C), 145.46 (2×C), 152.02 (C), 155.86 (C), 157.22 (C), 168.30 (C), 168.78 (C), 169.80 (C), 170.36 (C), 170.48 (C), 171.85 (C), 171.97 (C) ppm. HRMS [M+H] (EI): calcd $C_{81}H_{114}N_{15}O_{11}S$ 1504.85430; found 1504.85375.

4.2.10. Synthesis of peptide ***9****.* To peptide **7** (0.02 mmol, 0.03 g) trifluoroacetic acid (TFA) (0.70 mL) was added and the mixture was left stirring at room temperature for 5 h. The solvent was removed and the solid obtained was washed with an aqueous solution of EDTA 0.1 M and water. Peptide **9** (9.40 mg, 44%) was obtained as a green solid. ^{1}H NMR (400 MHz, DMSO): δ=0.74 (6H, br s, CH_3 Val), 1.60–1.64 (3H, m, βCH_2 Arg, $COCH_2CH_2$), 1.80–2.00 (4H, m, βCH_2 Arg, βCH Val, γCH_2 Arg), 2.00–2.15 (2H, m, CH_2CH_2-triazole), 2.15–2.27 (2H, m, $COCH_2CH_2$), 2.27–2.42 (2H, m, βCH_2 Asp), 2.73–2.86 (1H, m, βCH_2 Phe), 2.94–3.06 (1H, m, βCH_2 Phe), 3.07 (2H, m, δCH_2 Arg), 3.68 (2H, br s, CH_2 Gly), 4.10 (1H, br s, αCH Val), 4.26 (1H, br s, αCH Arg), 4.41–4.50 (3H, m, NHCH_2, αCH Asp), 4.56 (1H, br s, αCH Phe), 7.21–7.28 (7H, br s, ArH Phe, 2×NH), 7.30 (1H, s, CH), 7.88 (1H, s, CH), 8.07 (8H, m, 4×NH, ArH), 8.56 (1H, br s, NH), 8.66 (1H, br s, NH), 12.15 (1H, br s, CO_2H) ppm. ^{13}C NMR (100 MHz, DMSO): δ=17.34 (CH_2CH_2), 18.87 (CH_3 Val), 24.14 ($COCH_2CH_2$),

24.74 (γCH_2 Arg), 29.21 (βCH_2 Arg), 30.24 (βCH Val), 33.91 (COCH_2CH_2), 34.07 (NHCH_2), 36.08 (βCH_2 Asp), 37.75 (βCH_2 Phe), 40.38 (δCH_2 Arg), 41.93 (CH_2 Gly), 49.55 (αCH Asp), 52.52 (αCH Arg), 54.52 (αCH Phe), 58.02 (αCH Val), 120.42 (CH), 121.51 (CH), 121.13 (CH), 126.17 (CH Phe), 127.91 (CH Phe), 129.13 (CH Phe), 136.92 (C), 137.64 (C Phe), 146.00 (C), 147.61 (C), 155.44 (C=N), 168.60 (C=O), 170.30 (C=O), 170.76 (C=O), 170.93 (C=O), 171.86 (C=O), 171.93 (C=O), 172.18 (C=O) ppm. HRMS (EI): calcd $C_{41}H_{54}N_{15}O_8$ 884.42743; found 884.42699.

*4.2.11. Synthesis of peptide **10**.* To peptide **8** (55.70 μmol; 83.90 mg) TFA (0.60 mL) was added and the mixture was left stirring at room temperature for 6 h. The solvent was removed and the residue was treated with diethyl ether. Peptide **10** (59.40 mg, 81%) was isolated as a brown solid. ^{1}H NMR (400 MHz, DMSO): δ=0.51 (4H, br s, 2×CH_2), 0.68 (6H, t, J=4.8 Hz, 2×CH_3), 0.74 (6H, br s, 2×CH_3), 0.96 (12H, br s, 6×CH_2), 1.50 (3H, br s, βCH Arg, γCH_2 Arg), 1.68 (1H, br s, βCH Arg), 1.90–2.11 (15H, m, βCH, 7×CH_2), 2.26 (2H, br s, CH_2), 2.32 (2H, t, J=1.6 Hz, βCH_2), 2.69 (2H, br s, CH_2), 2.79 (1H, br s, βCH), 2.98–3.00 (1H, m, βCH), 3.09 (2H, dd, J 4.4 and 7.2 Hz, δCH_2 Arg), 3.71 (2H, br s, αCH_2), 4.13 (1H, br s, αCH), 4.30 (1H, br s, αCH), 4.40 (2H, br s, CH_2NH), 4.52 (1H, br s, αCH), 4.60 (1H, br s, αCH), 6.60 (3H, vbs, NH_3^+), 7.10–7.22 (5H, m, ArH Phe), 7.49 (2H, br s, 2×NH), 7.89 (2H, br s, 2×ArH), 8.02–8.05 (6H, m, 2×NH, 4×ArH), 8.10–8.20 (2H, m, 2×NH), 8.24 (1H, br s, NH), 8.56 (1H, br s, CH_2N*H*), 8.64 (1H, br s, CH), 8.69 (1H, br s, CH) ppm. ^{13}C NMR (100 MHz, DMSO): δ=13.74 (2×CH_3), 18.00 (CH_3), 19.05 (CH_3), 21.89 (2×CH_2), 23.32 (2×CH_2), 24.62 (CH_2), 24.89 (CH_2), 24.96 (γCH_2 Arg), 28.47 (2×CH_2), 28.97 (βCH_2 Arg), 30.37 (CH), 31.01 (2×CH_2), 34.01 (CH_2), 34.47 (CH_2), 36.17 (CH_2), 37.84 (CH_2), 39.08 (2×CH_2), 39.50 (2×CH_2), 39.71 (2×CH_2), 40.12 (δCH_2 Arg), 41.77 (CH_2), 49.68 (CH), 52.23 (CH), 54.20 (CH), 55.66 (C), 57.79 (CH), 114.24 (CH), 114.59 (CH), 118.77 (2×CH), 120.23 (CH), 121.19 (CH), 121.34 (2×CH), 126.19 (CH), 127.87 (CH), 129.16 (CH), 136.07 (C), 136.26 (C), 137.45 (C), 139.48 (C), 139.70 (C), 146.53 (C), 147.76 (C), 152.26 (2×C), 156.58 (C), 168.62 (C), 170.33 (C), 170.80 (C), 170.87 (C), 171.45 (C), 172.02 (C), 172.26 (C) ppm. HRMS [M+H] (EI): calcd $C_{64}H_{90}N_{15}O_8$ 1196.70913; found 1196.70913.

Acknowledgements

This work was supported by FEDER through the COMPETE Program (SCOMP-01-0124-FEDER-037302) and by the Portuguese Foundation for Science and Technology (FCT) in the framework of the Strategic Projects of CQ/UM [PEst-C/QUI/UI0686/2011 (FCOMP-01-0124-FEDER-022716)]. The NMR spectrometer Bruker Avance II 400 is part of the National NMR Network and was acquired with funds from FCT and FEDER. FCT is also acknowledged for the Ph.D. grant of H.V. (SFRH/BD/72651/2010) co-funded by the European Social Fund. The authors thank the access to the Minho University GRIUM Cluster and for contract research grant C2008-UMINHO-CQ-03.

References and notes

1. Marinelli, L.; Lavecchia, A.; Gottschalk, K.-E.; Novellino, E.; Kessler, H. *J. Med. Chem.* **2003**, *46*, 4393–4404.
2. Dayam, R.; Aiello, F.; Deng, J.; Wu, Y.; Garofalo, A.; Chen, X.; Neamati, N. *J. Med. Chem.* **2006**, *49*, 4526–4534.
3. Gottschalk, K.-E.; Kessler, H. *Angew. Chem., Int. Ed.* **2002**, *41*, 3767–3774.
4. Manzoni, L.; Belvisi, L.; Arosio, D.; Civera, M.; Pilkington-Miksa, M.; Potenza, D.; Caprini, A.; Araldi, E. M. V.; Monferini, E.; Mancino, M.; Podestà, F.; Scolastico, C. *ChemMedChem* **2009**, *4*, 615–632.
5. Mas-Moruno, C.; Rechenmacher, F.; Kessler, H. *Anti-Cancer Agents Med. Chem.* **2010**, *10*, 753–768.
6. D'Andrea, L. D.; Gatto, A.; Pedone, C.; Benedetti, E. *Chem. Biol. Drug Des.* **2006**, *67*, 115–126.
7. Casiraghi, G.; Rassu, G.; Auzzas, L.; Burreddu, P.; Gaetani, E.; Battistini, L.; Zanardi, F.; Curti, C.; Nicastro, G.; Belvisi, L.; Motto, I.; Castorina, M.; Giannini, G.; Pisano, C. *J. Med. Chem.* **2005**, *48*, 7675–7687.
8. Park, J.-A.; Lee, J.-J.; Jung, J.-C.; Yu, D.-Y.; Oh, C.; Ha, S.; Kim, T.-J.; Chang, Y. *ChemBioChem* **2008**, *9*, 2811–2813.
9. Wu, Y.; Zhang, X.; Xiong, Z.; Cheng, Z.; Fisher, D. R.; Liu, S.; Gambhir, S. S.; Chen, X. *J. Nucl. Med.* **2005**, *46*, 1707–1718.
10. Liu, S. *Mol. Pharmaceutics* **2006**, *3*, 472–487.
11. Gurrath, M.; Muller, G.; Kessler, H.; Aumailley, M.; Timpl, R. *Eur. J. Biochem.* **1992**, *210*, 911–921.
12. Haubner, R.; Gratias, R.; Diefenbach, B.; Goodman, S. L.; Jonczyk, A.; Kessler, H. *J. Am. Chem. Soc.* **1996**, *118*, 7461–7472.
13. Pierschbacher, M. D.; Ruoslahti, E. *J. Biol. Chem.* **1987**, *262*, 17294–17298.
14. Pfaff, M.; Tangemann, K.; Muller, B.; Gurrath, M.; Muller, G.; Kessler, H.; Timpl, R.; Engel, J. *J. Biol. Chem.* **1994**, *269*, 20233–20238.
15. Dechantsreiter, M. A.; Planker, E.; Matha, B.; Lohof, E.; Holzemann, G.; Jonczyk, A.; Goodman, S. L.; Kessler, H. *J. Med. Chem.* **1999**, *42*, 3033–3040.
16. Liu, Y.; Zhang, L.; Wan, J.; Li, Y.; Xu, Y.; Pan, Y. *Tetrahedron* **2008**, *64*, 10728–10734.
17. Rostovtsev, V. V.; Green, L. G.; Fokin, V. V.; Sharpless, K. B. *Angew. Chem., Int. Ed.* **2002**, *41*, 2596–2599.
18. Cantel, S.; Le Chevalier Isaad, A.; Scrima, M.; Levy, J. J.; DiMarchi, R. D.; Rovero, P.; Halperin, J. A.; D'Ursi, A. M.; Papini, A. M.; Chorev, M. *J. Org. Chem.* **2008**, *73*, 5663–5674.
19. Jagasia, R.; Holub, J. M.; Bollinger, M.; Kirshenbaum, K.; Finn, M. G. *J. Org. Chem.* **2009**, *74*, 2964–2974.
20. Tao, C.-Z.; Cui, X.; Li, J.; Liu, A.-X.; Liu, L.; Guo, Q.-X. *Tetrahedron Lett.* **2007**, *48*, 3525–3529.
21. Wu, Y.-M.; Deng, J.; Fang, X.; Chen, Q.-Y. *J. Fluorine Chem.* **2004**, *125*, 1415–1423.
22. Hancock, W. S.; Battersby, J. E. *Anal. Biochem.* **1976**, *71*, 260–264.
23. Wang, J.; Wolf, R. M.; Caldwell, J. W.; Kollman, P. A.; Case, D. A. *J. Comput. Chem.* **2004**, *25*, 1157–1174.
24. Hess, B.; Kutzner, C.; van der Spoel, D.; Lindahl, E. *J. Chem. Theory Comput.* **2008**, *4*, 435–447.
25. Schmidt, M. W.; Baldridge, K. K.; Boatz, J. A.; Elbert, S. T.; Gordon, M. S.; Jensen, J. H.; Koseki, S.; Matsunaga, N.; Nguyen, K. A.; Su, S.; Windus, T. L.; Dupuis, M.; Montgomery, J. A. *J. Comput. Chem.* **1993**, *14*, 1347–1363.
26. Berendsen, H. J. C.; Postma, J. P. M.; Van Gunsteren, W. F.; DiNola, A.; Haak, J. R. *J. Chem. Phys.* **1984**, *81*, 3684–3690.
27. Xiong, J.-P.; Stehle, T.; Zhang, R.; Joachimiak, A.; Frech, M.; Goodman, S. L.; Arnaout, M. A. *Science* **2002**, *296*, 151–155.
28. Morris, G. M.; Goodsell, D. S.; Halliday, R. S.; Huey, R.; Hart, W. E.; Belew, R. K.; Olson, A. J. *J. Comput. Chem.* **1998**, *19*, 1639–1662.